Hydrogel-Gate Graphene Field-Effect Transistors as Multiplexed Biosensors

Hamed Hosseini Bay[†], Richard Vo[†], Xiaochuan Dai[,†], Huan-Hsuan Hsu, Zhiming Mo, Siran Cao, Wenyi Li, Fiorenzo Omenetto, and Xiaocheng Jiang[*]*

Department of Biomedical Engineering, Tufts University, Medford, Massachusetts, 02155, United States

ABSTRACT

Nanoscale field-effect transistors (FETs) represent a unique platform for real time, label-free transduction of biochemical signals with unprecedented sensitivity and spatiotemporal resolution, yet their translation toward practical biomedical applications remains challenging. Herein, we demonstrate the potential to overcome several key limitations of traditional FET sensors by exploiting bioactive hydrogels as the gate material. Spatially-defined photopolymerization is utilized to achieve selective patterning of polyethylene glycol (PEG) on top of individual graphene FET devices, through which multiple bio-specific receptors can be independently encapsulated into the hydrogel-gate. The hydrogel-mediated integration of penicillinase has been demonstrated to effectively catalyze enzymatic reaction in the confined microenvironment, enabling real time, label-free detection of penicillin down to 0.2 mM. Multiplexed functionalization with penicillinase and acetylcholinesterase has been demonstrated to achieve highly specific sensing. In addition, the microenvironment created by the hydrogel-gate has been shown to significantly reduce the nonspecific binding of non-target molecules to graphene channels, as well as preserve the encapsulated enzyme activity for at least 1 week, in comparison to free enzymes showing significant signal loss within one day. This general approach presents a new biointegration strategy and facilitates multiplex detection of bioanalytes on the same platform which could underwrite new advances in healthcare research.

KEYWORDS

Bioelectronics / hydrogel / polyethylene glycol / physiological fluids / photopolymerization / projection lithography

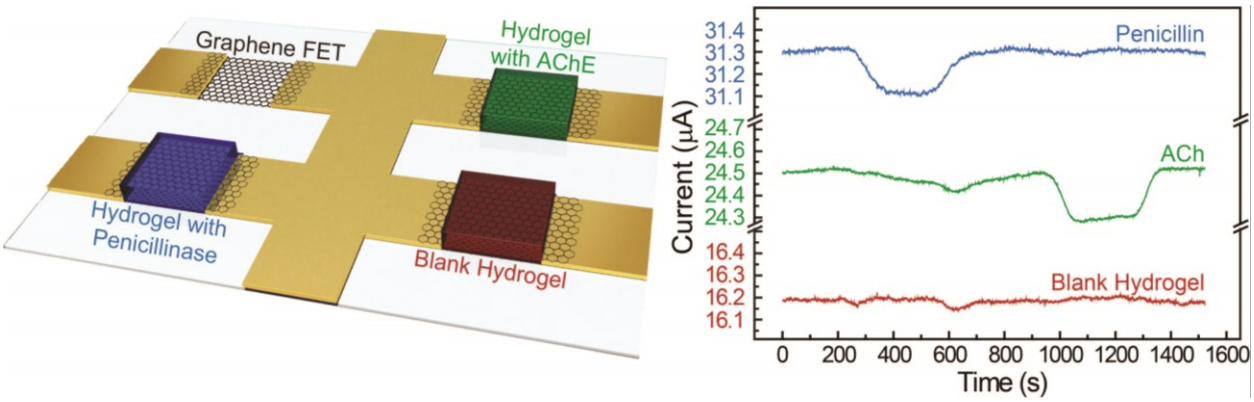

The optimal detection of biomolecules and their interactions represents a key to understanding, interrogating and directing many biologically significant processes. Nanoscale FETs have been exploited as label-free transducers for ultrasensitive biomolecular detection with unprecedented spatiotemporal resolution[1-3]. Different from traditional electrical/ electrochemical sensors which involves redox reactions between target molecules and electrodes and only work with certain electroactive species, nanoscale FETs function by detecting the variation of charge or electric potential at the surface and represent a more general and less invasive platform that could potentially work for all charged molecules. By functionalizing FET surface with biospecfic receptors, such as antibodies[4,5], enzymes[6,7], or single-strand DNA probes[8,9], selective binding to targeted biomolecules in solution could be achieved. The surface charges of target biomolecules, which are dependent on the isoelectric point, solution pH, or the charge transport induced by enzymatic reactions, will modulate the carrier density of FET channel and transduce the binding/unbinding events into electrical conductivity change in real time. Nanoscale FETs can be configured with a variety of semiconductor materials, including silicon nanowires[10,11], carbon nanotubes[3,12,13], graphene[13-16], and layered MoS_2[17]. Because of the comparable dimensions of nanomaterials (diameter or thickness) to most biomolecules and high surface-to-volume ratio, ultimate sensitivities have been demonstrated for protein disease biomarkers[4,7,15] (femtomolar level), nucleic acids[8,9,18] (tens of femtomolar level) as well as single viruses[5] and bacteria[18].

However, the translation of FET-based nanosensors for practical biomedical applications remains a challenge. The high-ionic strength in physiological environment makes the charged biomolecules undetectable as a result of Debye charge screening[19,20]. Additional desalting pretreatment has been used to remove ionic species from physiological fluids (such as blood serum, urine, etc.) and would compromise the real time sensing capability of FET[21]. In addition, the natural physiological environment contains a high concentration of proteins and other biomolecules at the level up to tens of mg/mL. This overwhelming background will cause significant nonspecific absorption and false-signal transduction on nanoscale FETs due to the increased surface area and superior sensitivity. This issue becomes particularly serious when carbon based nanomaterials, such as graphene or carbon nanotubes, are exploited as FET channels, as they are known for strong interaction with biomolecules through π-π stacking[22,23]. Moreover, most biospecific receptors, enzymes, have limited stability in the *in vitro* environment and would lose their activity quickly at room temperature after integration with FET devices.

Strategies need to be developed to better preserve these sensitive elements in local microenvironment without compromising device performance[24]. Hydrogel, a crosslinked three-dimensional polymeric network that retains a significant fraction of water, has been widely used for a range of biointerfacing applications. Particularly, PEG has been found to play important roles in modifying the local dielectric microenvironment on charge-based nanoelectronic biosensors to increase the effective Debye screening length and achieve real time label-free detection of biospecies under physiological relevant condition[20,23].

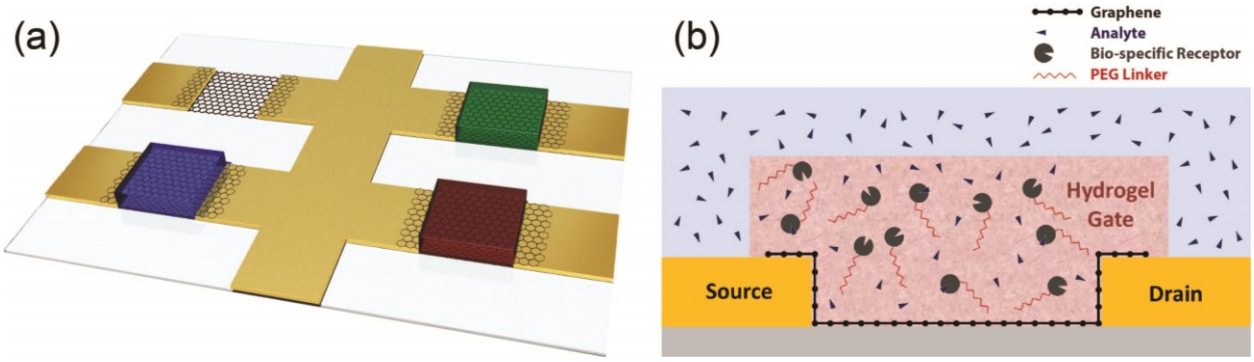

Figure 1. Schematic representation of (a) graphene FET device arrays with individually patterned biologically-encoded hydrogel-gates. Gold, electrode interconnects for the graphene FET devices. Black, graphene channels, Red, green and blue, specifically encoded hydrogel-gates. (b) PEGylated bioreceptor molecules encapsulated in biofunctional gates on graphene FET channels.

To this end, we exploited spatially-defined functional hydrogels as the interfacing material to develop a hybrid FET sensing platform that improves biosignal transduction at molecular level. As demonstrated schematically in Figure 1a, different biologically-encoded hydrogel-gates are individually patterned on top of graphene FET channels, through which different bio-specific receptors can be selectively encapsulated into these hydrogel "gates" to independently encode device selectivity for multiplexed real time molecular detection. The biofunctional hydrogels were formed by copolymerization of PEG linker/conjugated biomolecule complex and polyethylene glycol diacrylate (PEGDA) in presence of Eosin Y as photoinitiator to trigger covalent crosslinking and gelation. The creation of the hydrogel microenvironment in close proximity to graphene channels (Figure 1b) is expected to significantly extend the lifetime of sensitive bio-receptor/enzymes, reduce the nonspecific binding between graphene and non-target

bio-species, and modulate local dielectrics to mitigate charge-screening effect and enable real time sensing directly from the high-ionic strength physiological fluids without pre-processing.

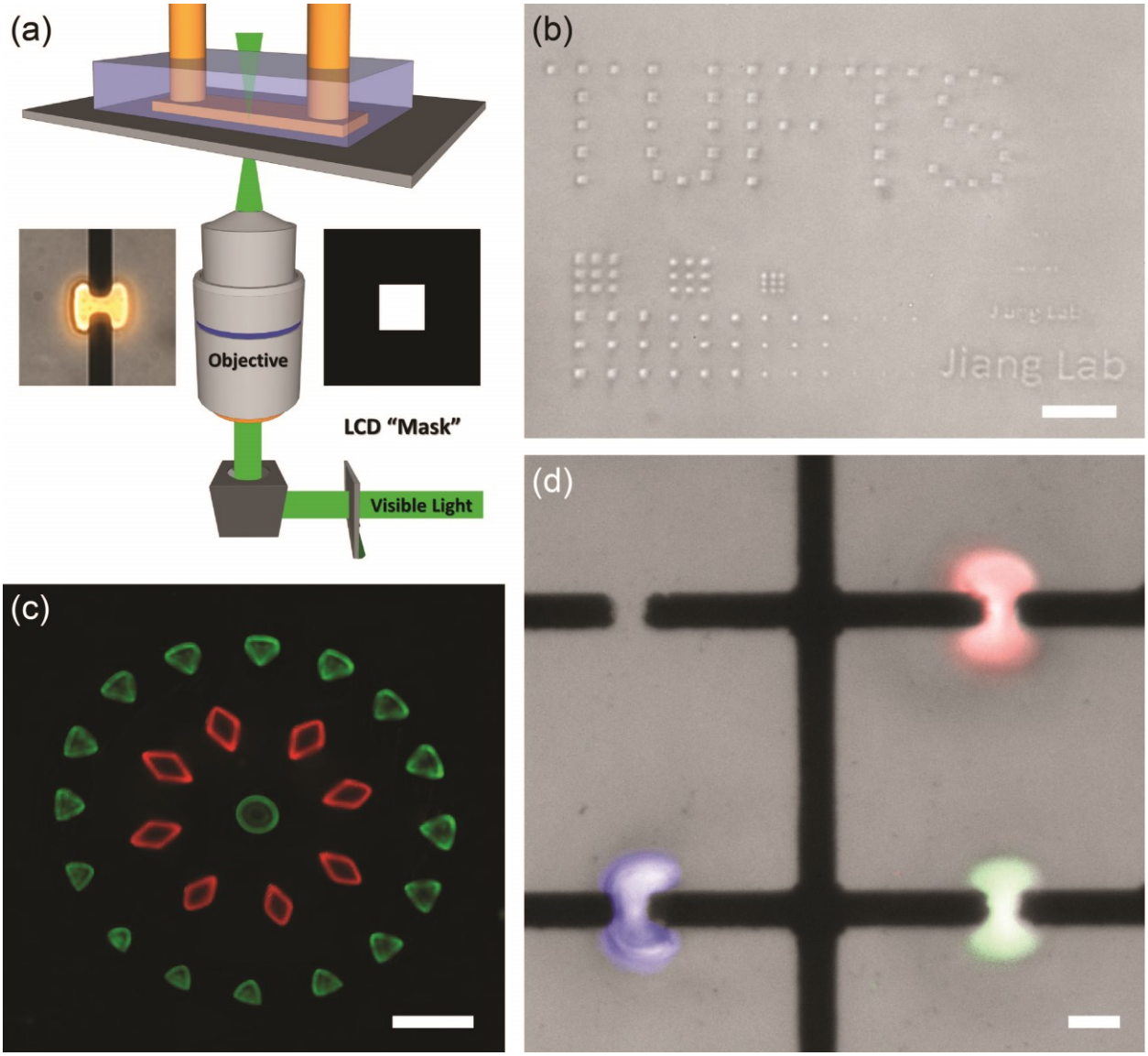

Figure 2. (a) Schematic representation of projection microlithography setup for biofunctional hydrogel patterning. (b) Bright field microscopic image demonstrating spatial resolution limit of patterned hydrogels with features down to ~1 μm, with the projection microlithography. Scale bar, 20 μm. (c) Fluorescence microscopic image of complex patterns of hydrogel with red and green fluorescent dyes. Scale bar, 250 μm. (d) Stacked bright field and fluorescence microscopic images of graphene FET array with hydrogel-gate highlighted with red, green and blue fluorescent dyes. Scale bar, 20 μm.

Our strategy involves a unique approach to directly functionalize specifically encoded hydrogels onto target FET channels through diffraction limited projection microlithography (Figure 2a). In brief, the microlithography system has been established with collimated light from a Zeiss inverted microscope filtered and masked by a LCD based spatial modulator; the LCD pattern is then demagnified and projected onto the bottom of device by microscope objectives[25]. The LCD mask can be easily programmed through computer interface, and hydrogel structures successfully formed with feature down to ~1 μm have demonstrated the diffraction limited photopolymerization[26] (Figure 2b). To enable the integration of multiple bio-receptors on the same platform, we have also developed microfluidic platforms (Figure 2a) for sequential delivery and polymerization of different monomer combinations, as demonstrated by the patterning of multi-fluorophores-encoded hydrogels[27] (Figure 2c). As a proof-of-concept, single layer graphene prepared by chemical vapor deposition[28] on copper foil was transferred onto photolithographically patterned gold electrodes and configured as FET channels[29] (Figure S1a). Then hydrogels-encoded with red, green and blue colored fluorescent dyes[27] conceptually representing multiplexed bio-receptors were patterned onto graphene channels with the projection microlithography setup (Figure 2d). These well-established hydrogel patterning techniques enable the precise and high-resolution integration of a broad spectrum of hydrogel materials to fulfill various biomedical needs[24].

The conductance of graphene FET biosensors exhibits pH value dependence. To characterize such dependence, a PDMS microfluidic channel was first aligned and bonded onto the as-fabricated FET sensors chip for varied buffer delivery[30]. Then, Ag/AgCl electrode was mounted as reference to enable liquid-gate measurements. Last, the FET sensor chip was connected to the data acquisition system using receptacle connector arrays (Figure S1b). By sequentially introducing buffer solution with different pH values into the microfluidic channels, the conductance of the graphene FET sensors can be quantitatively evaluated (Figure S2a). Specifically, increased conductance has been observed when the FET channel is subjected to higher pH value buffers, which indicates p-doping of the graphene FET without gate modulation. Independent signal values attributed to each pH value change was calculated according to liquid gate measurement (Figure S2b) and summarized in Figure S2c. The plot conveys a linear change of conductance with pH over the range from 6.2 to 8.2.

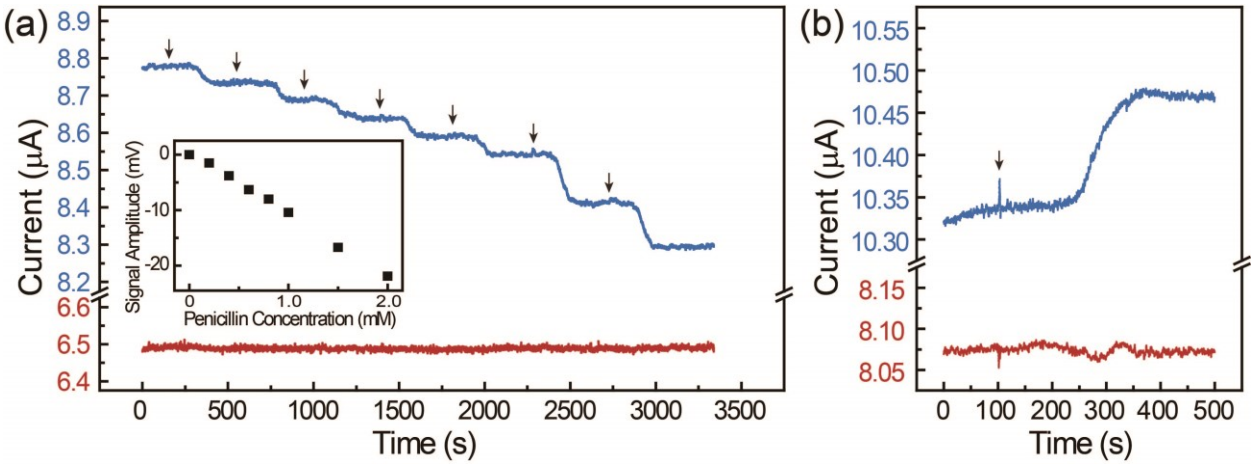

Figure 3. (a) Real time penicillin sensing. Blue and red traces represent penicillinase-encoded and blank hydrogel-gate FET channels, respectively. Arrows depict the time points chronologically of solution switching to buffer with 0.2 mM penicillin, 0.4 mM penicillin, 0.6 mM penicillin, 0.8 mM penicillin, 1.0 mM penicillin, 1.5 mM penicillin and 2.0 mM penicillin. Inset plot represent the correlation between signal amplitudes as a function of penicillin concentration in the buffer. (b) Blue and red traces represent bare graphene FET and hydrogel-gate FET channels, respectively, representing the nonspecific absorption of BSA is minimized with the existence of hydrogel-gate. Arrows show the time point of solution switching to buffer-BSA.

We initially tested the hydrogel-gate graphene FET as real time label-free biosensor for Penicillin G as a demonstrative analyte. In order to detect Penicillin G, aforementioned photopolymerization was carried out to selectively pattern bioactive PEG hydrogel encapsulating penicillinase[31] (Figure S1a, inset). The specific enzymatic reaction will generate penicilloic acid and cause local acidification within the hydrogel[32], resulting in a decrease in conductance of graphene FET biosensor. Real time recording of conductance changes (blue) while switching the same buffer with various concentration of Penicillin G from 0.2 mM to 2.0 mM demonstrates the sensing capability[33], in clear comparison with the stable conductance (red) simultaneously measured from control FET sensor with blank PEG hydrogel (Figure 3a). The measurements were carried out under a constant flow of the buffer solutions at a rate of 1.5 mL/h. Under such flow rate, it takes about 180 s for the exchanged solutions to reach FET devices. The signal voltage values from penicillin sensing were converted according to the transconductance of the bioactively gated device derived from liquid gate measurement and an almost linear trend is

observed in the presence of 0 to 2.0 mM analyte. (Figure 3a inset). Limit of detection (defined as 3 times standard deviation), although shows variation across different devices, has been experimentally testified below 200 μM, while it is capable to reach 50 μM estimated by interpolation.

Bovine Serum Albumin (BSA) was used as model system to assess the effect of hydrogel-gate on nonspecific absorption of biomolecules onto graphene FET channels, which is a critical shortfall on nanoscale FET biosensors. More than 50% of blood serum is consisted of Serum Albumin (SA) which signifies its role as a dominant source of false signal generation[34]. Simultaneous recording from bare graphene FET and graphene FET patterned with blank hydrogel-gate (Figure 3b) demonstrated that the conductance of bare graphene FET sensor (blue) depicts a 0.14 μA increase upon exposure of 100 μM BSA, corresponding to negatively charged BSA under pH value at 7.4[35]. Meanwhile no signal was generated from hydrogel-gate graphene FET sensor (red) which indicates the nonspecific adsorption of BSA on the graphene channel has been largely suppressed with the hydrogel passivation.

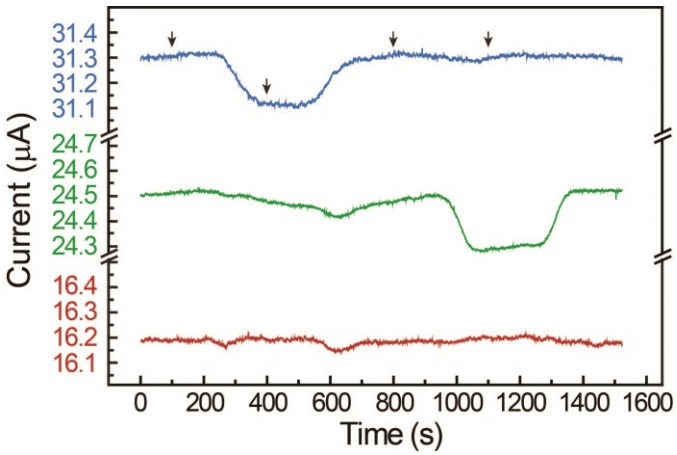

Figure 4. Real time multiplexed sensing of penicillin and acetylcholine chloride. Blue, green and red traces represent penicillinase-encoded, acetylcholinesterase-encoded and blank hydrogel-gate FET channels, respectively. Arrows depict the time points chronologically of solution switching to buffer-penicillin, buffer, buffer-acetylcholine, and buffer. After the analyte solution is switched into pure buffer, the device current rapidly returns to the original baseline, demonstrating the reversibility of sensing.

We chose penicillin and acetylcholine chloride to demonstrate the capability for multiplexed sensing with specifically encoded hydrogel-gate FET sensors (Figure 4). Simultaneous recording from graphene FET sensors with penicillinase-encoded hydrogel, acetylcholinesterase-encoded hydrogel and blank hydrogel has portrayed the specific signals upon introduction of different analytes (Figure 4). Buffer solution containing 3 mM Penicillin G solution was first introduced, leading to a conductance drop only in the penicillinase-encoded hydrogel-gate FET sensor (blue). Following a wash with pure buffer solution, another buffer solution with 1.5 mM acetylcholine chloride was subsequently introduced into the microfluidic channel which yields a conductance drop only in the acetylcholinesterase-encoded hydrogel-gate FET sensor (green). The lower conductivity as a result of enzymatic reaction between acetylcholinesterase and acetylcholine chloride can be associated with formation of carboxylic acid which deprotonates at neutral pH and increase the acidity of the local environment[32]. No signal was generated from the blank hydrogel-gate graphene FET sensor (red). Different hydrogel-gate FETs are 50-100 µm apart and signal transduction from each channel does not affect others. Hence, the enzymatic reactions are confined within the microenvironment formed by the biologically-encoded hydrogels, paving the way to the real time multiplexed detection of analytes with the same hydrogel-gate FET biosensor platform.

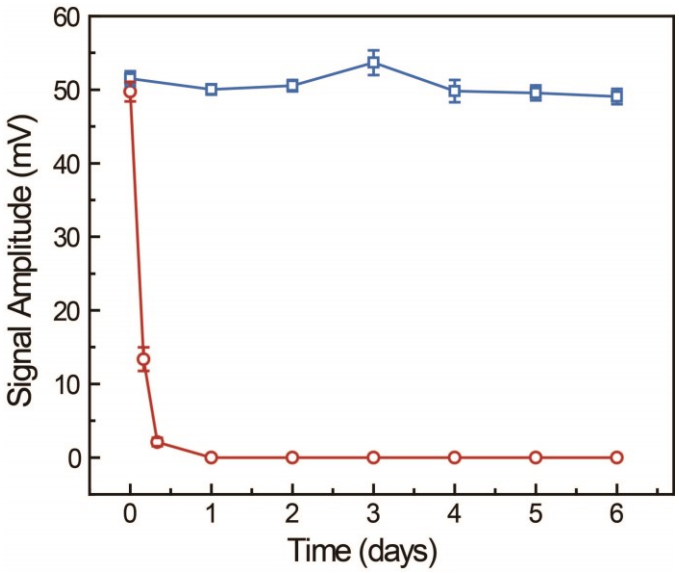

Figure 5. Absolute signal amplitudes measured from devices with hydrogel-encapsulated penicillinase (blue) and free penicillinase (red), representing enzyme activity changing over a week. Each measurement was repeated 3 times.

In addition to the specific and multiplexed detection of multiple analytes, it is also expected that the encapsulation of proteins and enzymes within the hydrogel microenvironment can extend their lifetime and preserve the activity. Proteins and enzymes have limited stability due to their relatively fast and progressive chemical and structural degradation in solutions[36]. Silk has been used to extend the shelf life of antibiotics, vaccines and enzymes by encapsulation to produce protective microenvironments, barriers, and immobilizing the protein structure to reduce protein unfolding[36,37]. Crosslinked PEG[38,39], alginate[40] and gelatin[41] hydrogels have also been reported to successfully entrap enzymes and antibodies in order to preserve their activity. Here, we expect the photopolymerized PEG can enhance the stability of enzymes in solution and preserve the high sensitivity of enzymatic reaction based nanoelectronic biosensor over an extensive period of time. As a proof-of-concept, the device sensitivity of graphene FET with penicillinase-encoded hydrogel-gate over time was assessed longitudinally with 10 mM Penicillin G as the analyte. A high concentration of 10 mM was chosen to avoid the penicillin concentration as the limiting factor of the enzymatic reaction and to show clearly the changes caused by any possible degradation or irreversible consumption of the enzymes. As illustrated in Figure 5, the analyte solution were periodically introduced to the chip while voltage signal amplitudes measured from three different devices and converted with individual transconductance of each device were recorded and plotted as a function of time for up to a week. Hydrogel-gate devices suffer no degradation of sensitivity over a week (blue), proving the significantly enhanced stability of enzyme molecules as well as minimal irreversible binding with the enzymes. As a control experiment, a stock solution of 1 mg/mL penicillinase has been used to evaluate the lifetime of the free enzyme, which showed ~70% loss of signal amplitude in less than 4 hours and no measurable activity within one day (red). The hydrogel encapsulation strategy offers an alternative approach to preserve the high sensitivity of multiplexed nanoelectronic biosensors based on enzymatic activity as well as protein bioreceptors[42].

In conclusion, we outline a novel and general strategy to overcome the common limitations of FET biosensing platforms by exploiting molecularly-encoded functional hydrogel as the gate material. Spatially-defined photopolymerization is utilized to achieve selective patterning of

hydrogel on top of individual graphene FET devices with diffraction-limited spatial resolution. Combined with on-chip microfluidic control, bio-specific receptors can be sequentially encapsulated into the hydrogel-gate to independently encode selectivity in FET device arrays. The hydrogel-mediated integration of penicillinase, for example, has been demonstrated to effectively catalyze enzymatic reaction in the confined FET microenvironment, enabling real time, label-free detection of penicillin down to 0.2 mM. When additional enzymes (such as acetylcholinesterase) are incorporated into adjacent devices, highly specific and localized signals can be recorded with minimal cross-talk, thus demonstrating the unique potential of the current strategy in high spatial resolution multiplex sensing. In addition, the passivation of the graphene FET device with a hydrogel layer is found to significantly reduce the nonspecific binding of analyte molecules to graphene. Lastly, from the longitudinal measurements of hydrogel FET performance, the controlled microenvironment preserve the enzyme activity for at least 1 week, in comparison to free enzymes showing a 70% signal loss after 4 hours. Our current demonstrations are mainly focused on detection of small molecules; for detection of larger molecules, the microstructure of hydrogel can be further tailored on demand, such as formulating meso- or macro-porous hydrogel structures via inclusion of inactive porogens during the photopolymerization process. Moving forward, this strategy can also be implemented for other semiconducting materials used as FET channel such as silicon nanowires, carbon nanotubes and transition metal dichalcogenides. The current work represents a strategic approach to enable the application of existing nanoelectronic tool sets in physiologically relevant conditions and has potential for use in real time point-of-care diagnostics and *in vivo* monitoring of disease progression through long-term tissue interfacing applications[43,44].

ASSOCIATED CONTENTS

Supporting Information

Additional information including figures showing device design, pH sensing, liquid gate measurements.

AUTHOR INFORMATION

Corresponding Author

*Email: Xiaocheng.Jiang@tufts.edu.

*Email: Xiaochuan.Dai@tufts.edu.

Author Contributions

† H.H.B., R.V., and X.D. contributed equally to this work.

Notes

The authors declare no competing financial interest.

ACKNOWLEDGMENT

This work was supported by National Science Foundation (NSF CBET- 1803907) and Air Force Office of Scientific Research (FA9550-18-1-0128).

REFERENCES

(1) Chen, A.; Chatterjee, S. Nanomaterials based electrochemical sensors for biomedical applications. *Chem. Soc. Rev.* **2013**, *42*, 5425-5438.

(2) Patolsky, F.; Lieber, C. M. Nanowire nanosensors. *Mater. Today* **2005**, *8*, 20-28.

(3) Kauffman, D. R.; Star, A. Electronically monitoring biological interactions with carbon nanotube field-effect transistors. *Chem. Soc. Rev.* **2008**, *37*, 1197-1206.

(4) Stern, E.; Klemic, J. F.; Routenberg, D. A.; Wyrembak, P. N.; Turner-Evans, D. B.; Hamilton, A. D.; LaVan, D. A.; Fahmy, T. M.; Reed, M. A. Label-free immunodetection with CMOS-compatible semiconducting nanowires. *Nature* **2007**, *445*, 519-522.

(5) Patolsky, F.; Zheng, G.; Hayden, O.; Lakadamyali, M.; Zhuang, X.; Lieber, C. M. Electrical detection of single viruses. *Proc. Natl. Acad. Sci. U. S. A.* **2004**, *101*, 14017-14022.

(6) Duan, X.; Li, Y.; Rajan, N. K.; Routenberg, D. A.; Modis, Y.; Reed, M. A. Quantification of the affinities and kinetics of protein interactions using silicon nanowire biosensors. *Nature nanotechnology* **2012**, *7*, 401-407.

(7) Zheng, G.; Patolsky, F.; Cui, Y.; Wang, W. U.; Lieber, C. M. Multiplexed electrical detection of cancer markers with nanowire sensor arrays. *Nat. Biotechnol.* **2005**, *23*, 1294-1301.

(8) Star, A.; Tu, E.; Niemann, J.; Gabriel, J. C.; Joiner, C. S.; Valcke, C. Label-free detection of DNA hybridization using carbon nanotube network field-effect transistors. *Proc. Natl. Acad. Sci. U. S. A.* **2006**, *103*, 921-926.

(9) Hahm, J.; Lieber, C. M. Direct Ultrasensitive Electrical Detection of DNA and DNA Sequence Variations Using Nanowire Nanosensors. *Nano Lett.* **2004**, *4*, 51-54.

(10) Cui, Y.; Wei, Q.; Park, H.; Lieber, C. M. Nanowire nanosensors for highly sensitive and selective detection of biological and chemical species. *Science* **2001**, *293*, 1289-1292.

(11) Yogeswaran, U.; Chen, S. M. A Review on the Electrochemical Sensors and Biosensors Composed of Nanowires as Sensing Material. *Sensors* **2008**, *8*, 290-313.

(12) Gao, C.; Guo, Z.; Liu, J. H.; Huang, X. J. The new age of carbon nanotubes: an updated review of functionalized carbon nanotubes in electrochemical sensors. *Nanoscale* **2012**, *4*, 1948-1963.

(13) Balasubramanian, K.; Kern, K. 25th anniversary article: label-free electrical biodetection using carbon nanostructures. *Adv. Mater.* **2014**, *26*, 1154-1175.

(14) Zhan, B.; Li, C.; Yang, J.; Jenkins, G.; Huang, W.; Dong, X. Graphene field-effect transistor and its application for electronic sensing. *Small* **2014**, *10*, 4042-4065.

(15) Myung, S.; Solanki, A.; Kim, C.; Park, J.; Kim, K. S.; Lee, K. B. Graphene-encapsulated nanoparticle-based biosensor for the selective detection of cancer biomarkers. *Adv. Mater.* **2011**, *23*, 2221-2225.

(16) Liu, Y.; Dong, X.; Chen, P. Biological and chemical sensors based on graphene materials. *Chem. Soc. Rev.* **2012**, *41*, 2283-2307.

(17) Sarkar, D.; Liu, W.; Xie, X.; Anselmo, A. C.; Mitragotri, S.; Banerjee, K. MoS(2) field-effect transistor for next-generation label-free biosensors. *ACS nano* **2014**, *8*, 3992-4003.

(18) Mohanty, N.; Berry, V. Graphene-based single-bacterium resolution biodevice and DNA transistor: interfacing graphene derivatives with nanoscale and microscale biocomponents. *Nano Lett.* **2008**, *8*, 4469-4476.

(19) Stern, E.; Wagner, R.; Sigworth, F. J.; Breaker, R.; Fahmy, T. M.; Reed, M. A. Importance of the Debye screening length on nanowire field effect transistor sensors. *Nano Lett.* **2007**, *7*, 3405-3409.

(20) Gao, N.; Zhou, W.; Jiang, X.; Hong, G.; Fu, T. M.; Lieber, C. M. General strategy for biodetection in high ionic strength solutions using transistor-based nanoelectronic sensors. *Nano Lett.* **2015**, *15*, 2143-2148.

(21) Stern, E.; Vacic, A.; Rajan, N. K.; Criscione, J. M.; Park, J.; Ilic, B. R.; Mooney, D. J.; Reed, M. A.; Fahmy, T. M. Label-free biomarker detection from whole blood. *Nature nanotechnology* **2010**, *5*, 138-142.

(22) Chen, R. J.; Bangsaruntip, S.; Drouvalakis, K. A.; Kam, N. W.; Shim, M.; Li, Y.; Kim, W.; Utz, P. J.; Dai, H. Noncovalent functionalization of carbon nanotubes for highly specific electronic biosensors. *Proc. Natl. Acad. Sci. U. S. A.* **2003**, *100*, 4984-4989.

(23) Gao, N.; Gao, T.; Yang, X.; Dai, X.; Zhou, W.; Zhang, A.; Lieber, C. M. Specific detection of biomolecules in physiological solutions using graphene transistor biosensors. *Proc. Natl. Acad. Sci. U. S. A.* **2016**, *113*, 14633-14638.

(24) Seliktar, D. Designing cell-compatible hydrogels for biomedical applications. *Science* **2012**, *336*, 1124-1128.

(25) A custom-built projection lithography system was assembled. The system consists of an inverted microscope, projector, and a LCD “mask.” Devices were mounted onto the inverted microscope (AxioObserver Z1, Zeiss). A custom slider was 3D printed to hold the LCD in place. The LCD was then connected to the projector. The patterns of light exposure were

changed using a computer connected with the projector, which are then de-magnified through the inverted microscope onto the substrate.

(26) A solution of 50% monomer solution, 50% 300 mM L-cysteine, saturated with UV initiator (Irgracure, Sigma) was used for photopolymerization. The monomer solution was made by mixing PEGDA with co-initiators 1-vinyl-2-pyrrolidinone 99% (VP) (Sigma, 201-800-4) and triethanolamine (TEA) (Sigma, 90279) with ratios of 77.45%, 15.15% and 7.41% w/v, respectively. All solutions were prepared using deionized water. The mixture was introduced into the microfluidic channel followed by photopolymerization using UV light. The channel was washed with deionized water and the system was kept under constant flow.

(27) Red fluorescent dye (rhodamine g) concentration was adjusted at 30 ug/mL, and the aqueous stock solutions of blue (19774-10, Fluoresbrite) and green (16662-10, Fluoresbite) fluorescent microparticles were diluted to accommodate 4.55×10^{12} particles/mL. The solution containing one fluorescent dye was diluted to 10% by the photopolymerization solution mixture prior to being introduced into the microfluidic channel.

(28) Single layer graphene was synthesized via Chemical Vapor Deposition (CVD) using 25 μm thick copper foils as catalyst. Copper foil was cleaned with acetone and isopropanol and electropolished as anode using a mixture of ortho-phosphoric acid and ethylene glycol (3:1) against a copper counter electrode. Electropolished copper foil substrate was then rinsed thoroughly with deionized water and isopropanol and fully dried prior to graphene growth, prior to being loaded into the CVD. High purity Ar is purged into CVD chamber to reach 50 torr. The CVD reactor was then heated up to 850 °C with the rate of 40 °C/min. The foil was annealed at 850°C under Ar and H_2 (4:1) to reduce any surface oxides and achieve larger copper grains. Subsequently, graphene is synthesized using 40 sccm CH_4 as carbon precursor in 160 sccm H_2 atmosphere at 25 torr. The reactor was finally cooled down rapidly to room temperature under Ar and H_2 atmosphere. After synthesis, graphene was coated with poly(methyl methacrylate) (PMMA) and the protective PMMA layer was baked and hardened on a hotplate at 120 °C for 1 min.

(29) Metal interconnects were patterned through photolithography on a 35×50×0.16 mm glass coverslip substrates, following which Cr/Au (5 nm/30 nm) was deposited by thermal

evaporation. The substrates were later lifted-off in acetone. Graphene grown on copper foil was put into 0.2 M ammonium persulfate aqueous solution to etch copper foil leaving graphene/PMMA floating on the surface of solution. Graphene/PMMA was washed thoroughly with deionized water, transferred onto metal interconnects and baked at 200 °C for 1 h, prior to PMMA removal with acetone. FET channel arrays were patterned via photolithography and excess graphene was removed by oxygen plasma etching (75 W and 1 min).

(30) Microfluidic channels were fabricated by pouring polydimethylsiloxane (PDMS) on a silicon wafer. After curing, PDMS was cut using a scalpel and 1.5 mm holes were punched at each end to form the inlet and outlet of the microfluidic channels. PDMS was attached to the device via Kapton tape that was cut to form the channel. The PDMS channel was then sealed using epoxy. Polyethylene tubing was attached and glued to the PDMS channel as inlet and outlet for delivery and exchange of solutions. Ag/AgCl electrode was incorporated in the microfluidic channel and used as reference electrode to enable liquid-gate measurements. The FET sensing chip was connected to the data acquisition system using receptacle connector arrays during electrical measurement.

(31) Bioreceptor molecules (penicillinase and acetylcholinesterase) were covalently functionalized by incubating 10 μL of 50–200 μg/μL bioreceptor solution with 10 μL of 50–200 μg/μL solution of 2 KDa heterobifunctional PEG linker (ACRL-PEG-SVA) for 1 h at room temperature. PEGylated bioreceptors was mixed with monomer solution and Eosin Y disodium solution (5.0 mg/mL) with ratios of 48.75%, 50% and 1.25%, respectively. All solutions were prepared using 1X phosphate buffered saline. The mixture was introduced into the microfluidic channel followed by photopolymerization using visible light (514 nm). The channel was washed with PBS and the system was kept under constant flow. Flow rate ranging from 0.5-5.0 mL/h was tested to make sure the photopolymerized hydrogel-gate is stable under different flow rate.

(32) Mu, L.; Droujinine, I. A.; Rajan, N. K.; Sawtelle, S. D.; Reed, M. A. Direct, rapid, and label-free detection of enzyme-substrate interactions in physiological buffers using CMOS-compatible nanoribbon sensors. *Nano Lett.* **2014**, *14*, 5315-5322.

(33) Phosphate buffer solution was made by dissolving monosodium phosphate, disodium phosphate and sodium chloride in deionized water; hydrochloric acid or sodium

peroxide solution was used to adjust pH value to 7.4. Analyte solutions were prepared by dissolving penicillin or acetylcholine chloride in the aforementioned buffer solution. 2 mM phosphate and 5 mM sodium chloride buffer was used in the penicillin concentration dependence measurement and the PSA nonspecific absorption recording. 10 mM phosphate and 250 mM sodium chloride buffer was used in the multiplexed sensing experiment of penicillin and acetylcholine chloride. Constant 1.5 mL/h flow rate was used for all sensing experiments.

(34) Khatayevich, D.; Page, T.; Gresswell, C.; Hayamizu, Y.; Grady, W.; Sarikaya, M. Selective detection of target proteins by peptide-enabled graphene biosensor. *Small* **2014**, *10*, 1505-1513, 1504.

(35) Ohno, Y.; Maehashi, K.; Yamashiro, Y.; Matsumoto, K. Electrolyte-gated graphene field-effect transistors for detecting pH and protein adsorption. *Nano Lett.* **2009**, *9*, 3318-3322.

(36) Pritchard, E. M.; Dennis, P. B.; Omenetto, F.; Naik, R. R.; Kaplan, D. L. Review physical and chemical aspects of stabilization of compounds in silk. *Biopolymers* **2012**, *97*, 479-498.

(37) Tao, H.; Marelli, B.; Yang, M.; An, B.; Onses, M. S.; Rogers, J. A.; Kaplan, D. L.; Omenetto, F. G. Inkjet Printing of Regenerated Silk Fibroin: From Printable Forms to Printable Functions. *Adv. Mater.* **2015**, *27*, 4273-4279.

(38) Le Goff, G. C.; Srinivas, R. L.; Hill, W. A.; Doyle, P. S. Hydrogel microparticles for biosensing. *Eur. Polym. J.* **2015**, *72*, 386-412.

(39) Appleyard, D. C.; Chapin, S. C.; Doyle, P. S. Multiplexed protein quantification with barcoded hydrogel microparticles. *Anal. Chem.* **2011**, *83*, 193-199.

(40) Yahsi, A.; Sahin, F.; Demirel, G.; Tumturk, H. Binary immobilization of tyrosinase by using alginate gel beads and poly(acrylamide-co-acrylic acid) hydrogels. *Int. J. Biol. Macromol.* **2005**, *36*, 253-258.

(41) Truong, V. X.; Tsang, K. M.; Forsythe, J. S. Nonswelling Click-Cross-Linked Gelatin and PEG Hydrogels with Tunable Properties Using Pluronic Linkers. *Biomacromolecules* **2017**, *18*, 757-766.

(42) Kuchler, A.; Yoshimoto, M.; Luginbuhl, S.; Mavelli, F.; Walde, P. Enzymatic reactions in confined environments. *Nature nanotechnology* **2016**, *11*, 409-420.

(43) Zhang, A.; Lieber, C. M. Nano-Bioelectronics. *Chem. Rev.* **2016**, *116*, 215-257.

(44) Dai, X.; Hong, G.; Gao, T.; Lieber, C. M. Mesh Nanoelectronics: Seamless Integration of Electronics with Tissues. *Acc. Chem. Res.* **2018**, *51*, 309-318.